

# Non-Intrusive Electric Load Monitoring Approach Based on Current Feature Visualization for Smart Energy Management

Yiwen Xu, *Member, IEEE*, Dengfeng Liu, Liangtao Huang, Zhiqian Lin, Tiesong Zhao, *Senior Member, IEEE*, and Sam Kwong, *Fellow, IEEE*

**Abstract**—The state-of-the-art smart city has been calling for an economic but efficient energy management over large-scale network, especially for the electric power system. It is a critical issue to monitor, analyze and control electric loads of all users in system. In this paper, we employ the popular computer vision techniques of AI to design a non-invasive load monitoring method for smart electric energy management. First of all, we utilize both signal transforms (including wavelet transform and discrete Fourier transform) and Gramian Angular Field (GAF) methods to map one-dimensional current signals onto two-dimensional color feature images. Second, we propose to recognize all electric loads from color feature images using a U-shape deep neural network with multi-scale feature extraction and attention mechanism. Third, we design our method as a cloud-based, non-invasive monitoring of all users, thereby saving energy cost during electric power system control. Experimental results on both public and our private datasets have demonstrated our method achieves superior performances than its peers, and thus supports efficient energy management over large-scale Internet of Things (IoT).

**Index terms**— Smart City, Smart Electric Energy Management, Electric Load Monitoring, Load Recognition Algorithm, Computer Vision

## I. INTRODUCTION

THE past decades have witnessed a booming of urban populations with ever-increased municipal facilities to serve all citizens. An effective solution to manage these facilities is smart city with Internet of Things (IoT), which is mostly benefitted from the recent development of Artificial Intelligence (AI) [1]–[3]. To support the smart city, an economic but efficient electric power management system is indispensable [4]. A cloud-end administrator monitors electricity consumptions of all users and loads, presents analyses of all electricity usages, and provides advices to users or directly manages electricity usage of all loads. As a result, the overall electricity

This work is supported by the National Natural Science Foundation of China (No. 62171134) and Foundation for Middle-aged and Young Educational Committee of Fujian Province (No. JAT200024).

Y. Xu is with Fujian Key Lab for Intelligent Processing and Wireless Transmission of Media Information, Fuzhou University, China and also with Zhicheng College, Fuzhou University, China (e-mail: xu\_yiwen@fzu.edu.cn).

D. Liu, L. Huang and Z. Lin are with Fujian Key Lab for Intelligent Processing and Wireless Transmission of Media Information, Fuzhou University, China (e-mail: {221120036, 21112010, N191127023}@fzu.edu.cn).

T. Zhao is with Fujian Key Lab for Intelligent Processing and Wireless Transmission of Media Information, Fuzhou University, China, and also with Peng Cheng Laboratory, China (e-mail: t.zhao@fzu.edu.cn).

S. Kwong is with the Department of Computer Science, City University of Hong Kong, Kowloon, Hong Kong SAR (e-mail: cssamk@cityu.edu.hk).

consumptions are saved to support sustainable developments of cities and environments.

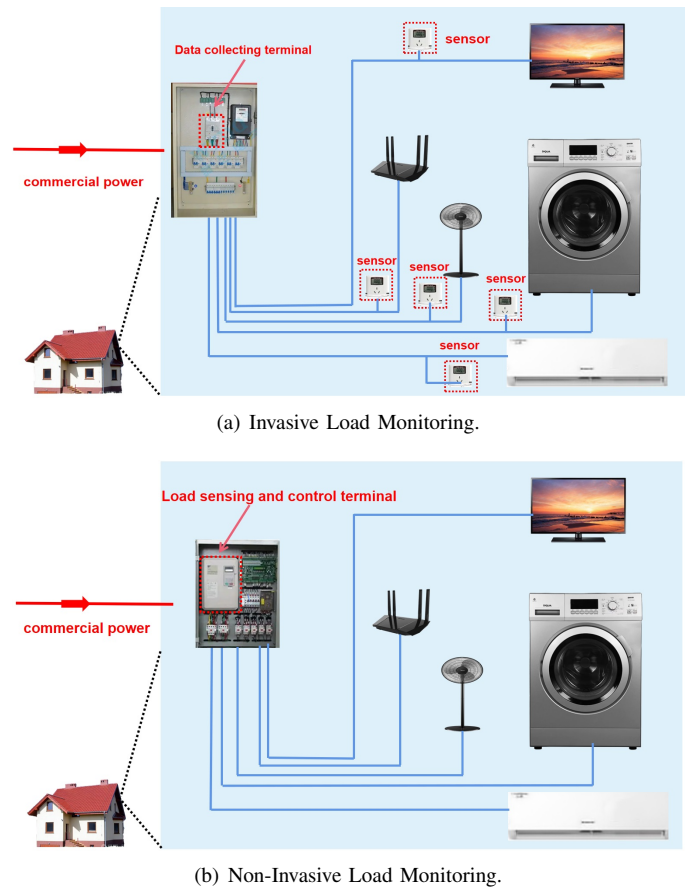


Fig. 1. The differences between invasive and non-invasive load monitoring in the electricity grid.

An efficient electric power management system is dependent on its electric load monitoring module [5]–[7], which can be realized by invasive or non-invasive approaches. In Invasive Load Monitoring (ILM), each electric load is monitored by a separate sensor and the information acquired from all sensors can be centrally processed by cloud-end. While in Non-Invasive Load Monitoring (NILM) [6]–[8], only one monitor is required for each family or cell. It captures electric signals (such as voltage, current, and so on) at the commercial power

input and transmits them to cloud server in which workload information of all loads are interpreted with algorithms. These differences can be shown in Fig. 1. Apparently, the non-invasive method is preferable in smart city infrastructure for its simple design, energy-efficient and low setup/maintenance cost.

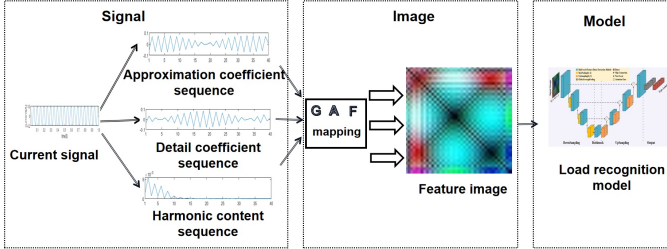


Fig. 2. The overall framework of the proposed LRA.

In the non-invasive design of Fig. 1 (b), Load Recognition Algorithm (LRA) plays an essential role and thus attracts attentions from researchers. Their contributions will be elaborated in Section II. Despite of these great efforts, there still exists a need to further improve the accuracy of LRA. Generally, load recognition may lead to inaccurate results when using inappropriate feature extraction, or false rejecting loads under masking effect – features of low power load are usually hard to be identified under high power loads. To address these issues, this paper presents a NILM method based on current feature visualization and a U-shape deep neural network for recognition. Our contributions are summarized as follows.

First, we propose a current feature visualization method based on signal transforms and Gramian Angular Field (GAF). By this operation, the feature differences between loads are highlighted to make ease of vision-based recognition.

Second, we propose a U-shape deep neural network based on multi-scale feature extraction and attention mechanism. This design aims to further enhance the recognition accuracies and generalization abilities of our method, especially at low power conditions.

Third, our NILM approach demonstrates its high efficiency in both public and our private datasets. To examine the generalization ability of proposed approach, we introduce a new dataset with 12 types of electric loads with powers from 24W to 1800W. Experimental results in this dataset as well as the public PLAID dataset validate our design.

The rest of paper is organized as follows. Section II reviews the related work on load monitoring. Sections III presents our contributions in current feature visualization and load recognition based on deep neural networks. Comprehensive experiments and analyses are presented in Section IV. Finally, Section V concludes this paper.

## II. RELATED WORKS

As pointed out in Section I, in a NILM method, only one terminal is deployed at the access point of family/cell. It sees the electrical loads in room within a black box. How to design

an effective LRA model to recognize or interpret these loads is thus critical.

Traditional LRA methodologies compared the feature of an unknown load with those of known loads in dictionary. They made judgments through a metric set consisting of matching degree [9], similarity degree [10], Hellinger distance [11], etc. The performance of LRA was also benefited from the development of machine learning, resulting in recognition methods with K-means clustering [12] and fuzzy C-means [13]. However, these methods basically utilized single feature without consideration on subtle differences between similar signals. Therefore, the problem of recognition confusion was not well addressed.

Researchers considered to introduce more types of signal features to improve the accuracy of LRA. [14] proposed a load recognition model with a feature combination of transient waveform and power change value during load switching. Kang *et al.* [15] employed fast Fourier transform to extract the amplitude and phase of odd harmonics of the current, and then used them as key features for recognition. To improve the recognition accuracies of loads, [16] constructed a hybrid feature set by the parameters of active power, reactive power and harmonic amplitude.

In the past decade, deep learning has demonstrated its strengths in AI-driven tasks, such as computer vision, natural language processing, human-computer interaction, and IoT. These successes also inspired the researchers to introduce deep neural networks in LRA. [17] designed a sequence-to-sequence Long-Short-Term Memory (LSTM) network for load recognition. The authors in [18] designed a capsule-network-based LRA, in which Convolutional Neural Network (CNN) extracted latent features from a set of non-overlapping energy measurement data segments. [19] proposed a dual-stream neural network to extract features from current signals. [20] proposed to extract features with Siamese neural networks and then used them in load recognition. These works have revealed the strong feature extraction abilities of neural networks with promising performance in load recognition.

To further promote the LRA accuracy, researchers also attempted to visualize the features of voltage or current and then employed image-alike processing techniques in load recognition. Owing to the advantage of recent booming of computer vision technologies, more accurate and robust LRA methods were developed. [21] presented an image-classification-based LRA, where the image was obtained with voltage-current (V-I) trajectory. [22] provided a CNN-based LRA with weighted pixel V-I trajectory map as features. Liu *et al.* employed color-coded V-I trajectory map as the input of their AlexNet-based load recognition model [23]. In [24], the V-I trajectory and amplitudes of current and voltage were mapped as a color image, which provided richer feature information to CNN-based load recognition. Wenninger *et al.* [25] mapped a cycle of V-I trajectories as a threshold-free recursive graphs, and subsequently designed a Spatial Pyramid Pooling (SPP) convolutional neural network for load recognition.

Our proposed method is also an image-based recognition approach that maps current features and employs image-alike recognition. Compared with its peers, we design a more

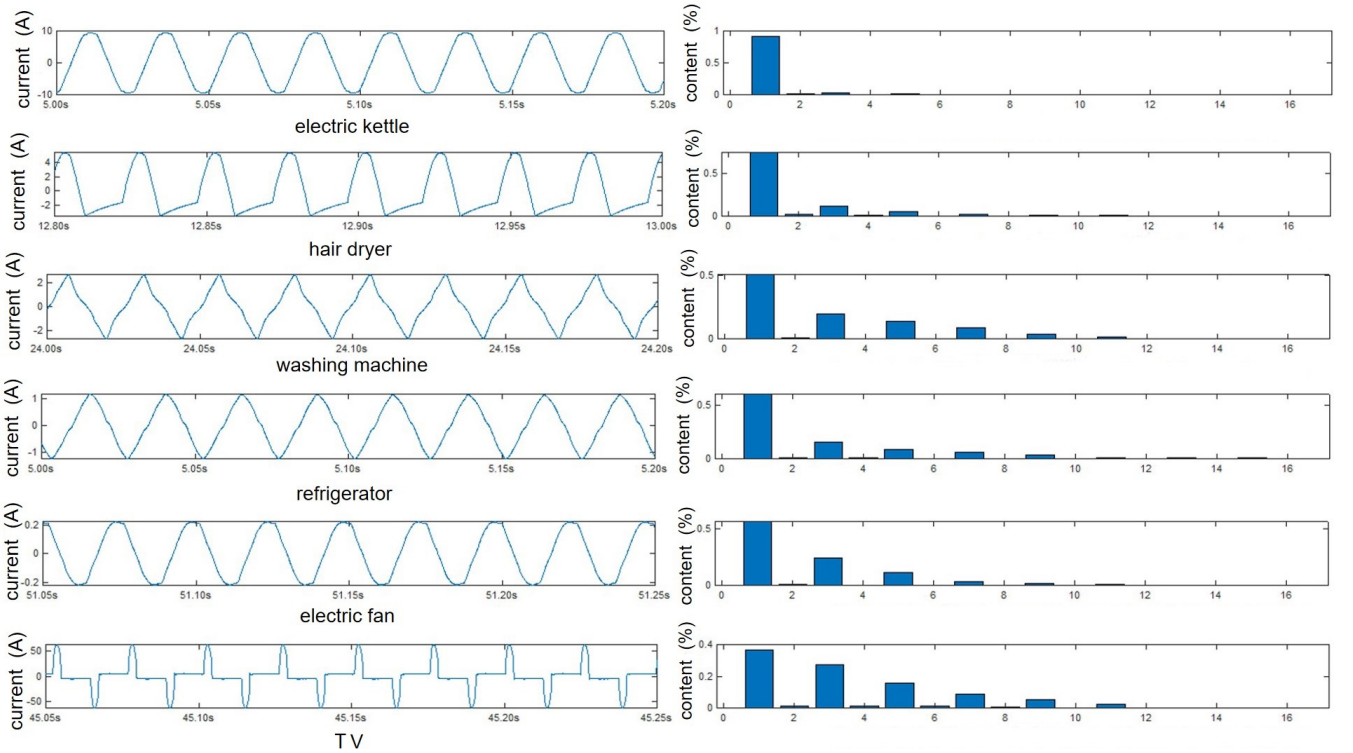


Fig. 3. Current signals and harmonic contents of typical loads.

effective feature mapping framework and a more reliable deep neural network for load recognition. Experimental results validate its design.

### III. PROPOSED METHOD

#### A. Motivation and Our Framework

By summarizing the above analysis in Section II, we expect to design an effective LRA method for NILM using more detailed, visualized features and a finely-optimized deep neural network. Among them, more detailed and visualized features benefit load recognition, especially for similar loads and low-power loads masked by high-power loads. The finely-optimized deep neural network helps to improve the accuracy of LRA.

Inspired by this, we propose a NILM method based on current feature visualization and deep neural network, as shown in Fig. 2. First of all, we employ wavelet and Discrete Fourier Transform (DFT) transform to decompose the current signal into three feature sequence: (i) approximation coefficient sequence with envelope feature of the current signal; (ii) detail coefficient sequence with texture feature of the current signal; (iii) harmonic ratio sequence with harmonic feature of the current signal. After that, we utilize the GAF method to convert the above three sequences into gray-scale images, and further set them as R, G, B channels of a color image. By this operation, the differences between loads are highlighted to make ease of load recognition. Finally, we propose a load recognition model based on multi-scale features and visual attention mechanism. These steps will be elaborated as follows.

#### B. Proposed Current Feature Visualization

In a NILM system, the terminal at commercial power input is able to capture the voltage and current signals. Between them, the voltage keeps almost intact while the current fluctuates with the electric usage on loads. Therefore, we select the current signal as the input of our load recognition model. To visualize the current signal as a two-dimensional image, we first extract its features and then convert them into gray-scale images, which are further set as channels of the visualized color image.

Denote the current signal by  $c(n)$  with a length  $N$ . It can be expanded into wavelet series as [26]:

$$c(n) = \frac{1}{\sqrt{N}} \sum_k W_\varphi(j_0, k) \cdot \varphi_{j_0, k}(n) + \frac{1}{\sqrt{N}} \sum_{j=j_0}^{\infty} \sum_k W_\psi(j, k) \cdot \psi_{j, k}(n), \quad (1)$$

where  $j$  represents wavelet decomposition scale that determines the length of wavelet coefficient,  $k$ .  $\varphi_{j_0, k}(n)$  and  $\psi_{j_0, k}(n)$  represent the scaling and wavelet functions, respectively.  $W_\varphi(j_0, k)$  and  $W_\psi(j, k)$  are approximation coefficient and detail coefficient, respectively. For ease of presentation, we denote them as  $S_a(n)$  and  $S_d(n)$ ,  $n = 0, 1, 2, \dots, N-1$ . They are calculated as [27]:

$$S_a(n) = \frac{1}{\sqrt{N}} \sum_n c(n) \varphi_{j_0, k}(n), \quad (2)$$

$$S_d(n) = \frac{1}{\sqrt{N}} \sum_n c(n) \psi_{j, k}(n), j > j_0. \quad (3)$$

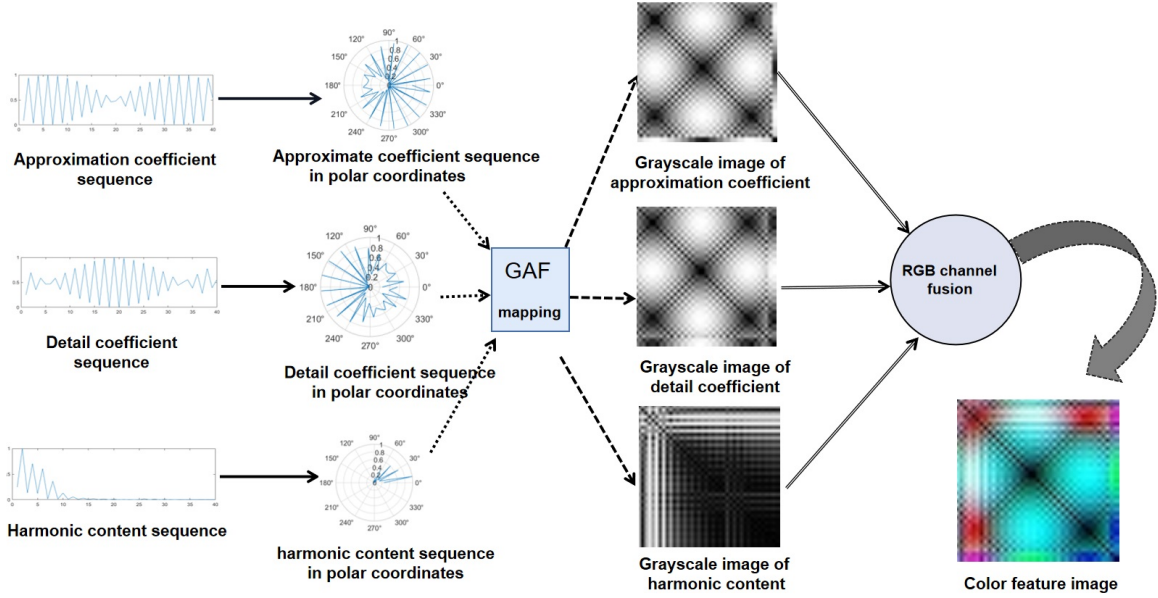


Fig. 4. Flowchart of our proposed current feature visualization method.

According to [28],  $S_a(n)$  and  $S_d(n)$  represent the envelope feature and texture feature of the current signal, respectively. This paper uses them as two features that will be visualized and recognized.

Another feature used in this paper is harmonic content which refers to the percentage of the  $k$ -th order harmonic component in the total harmonic components. As the  $k$ -th order harmonic component of the current signal can be obtained by DFT [29]:

$$r(k) = \frac{1}{N} \sum_{n=1}^N c(n) e^{-j \frac{2\pi k}{N} n}. \quad (4)$$

the harmonic content (denoted by  $S_h(k)$ ) is formulated as:

$$S_h(k) = \frac{r(k)}{\sum_{i=1}^N r(i)}. \quad (5)$$

The harmonic contents of loads vary subject to electrical components and circuit systems. To verify the above assumption, we explored the harmonic contents of different types of loads: resistive, pump-driven, motor-driven and switching-powered. The results are shown in Fig. 3 where the left part shows the current waves while the right part shows their corresponding harmonic contents. From this figure, the resistive loads (*e.g.* electric kettle, hair dryer) heat with resistors and barely have harmonic components. The pump-driven loads (*e.g.* washing machine, refrigerator) works mainly with fundamental wave, but with more 3rd, 5th and 7th harmonic components. The motor-driven loads (*e.g.* electric fan) are similar to pump-driven loads. They have 3rd, 5th, 7th and 9th harmonic components that are lower than fundamental wave. The switching-powered loads (*e.g.* TV, computer) adjust output voltages with high-frequency switches. They generate rich high-order harmonic components, such as 3rd, 5th, 7th, 9th, 11th and 13th harmonic components, which are comparable

with fundamental wave. Obviously, the harmonic content, *i.e.*  $S_h(k)$ , is an effective feature to identify different types of loads.

We then map all extracted features of  $S_a(n)$ ,  $S_d(n)$  and  $S_h(k)$  into grayscale images with GAF method. Take  $S_a(n)$  for example. Firstly,  $S_a(n)$ ,  $n = 0, 1, 2, \dots, N - 1$  are transferred from Cartesian coordinate system to polar coordinate system:

$$\begin{cases} \varphi(n) = \arctg[S_a(n)] \\ r(n) = \sqrt{S_a^2(n) + n^2} \end{cases}. \quad (6)$$

Then, an  $n \times n$  Gramian matrix  $\mathbf{G}_a$  is obtained in which

$$\mathbf{G}_a(i, j) = \sin(\varphi(i - 1) - \varphi(j - 1)). \quad (7)$$

Similarly, we also obtain the Gramian matrixes of  $S_d(n)$  and  $S_h(k)$ , respectively denoted by  $\mathbf{G}_d$  and  $\mathbf{G}_h$ . We use the following equations to map these Gramian matrixes to the R, G and B channels of a color image:

$$\begin{cases} \mathbf{R} = |\mathbf{G}_a| \times 255 \\ \mathbf{G} = |\mathbf{G}_d| \times 255 \\ \mathbf{B} = |\mathbf{G}_h| \times 255 \end{cases} \quad (8)$$

$$\mathbf{I}_F = [\mathbf{R} \ \mathbf{G} \ \mathbf{B}]. \quad (9)$$

The flowchart of our proposed current feature visualization can be summarized in Fig. 4. The fused color image,  $\mathbf{I}_F$ , with a resolution of  $40 \times 40$ , has its unique texture information and chroma components. It includes low-frequency envelope features, high-frequency texture details and all harmonic ratios. Compared with the original one-dimensional current signal, it visualized and highlighted all hidden features whilst keeping timestamp of the original signal. As a result, we are allowed to use CNN methods to recognize all loads with a high accuracy.

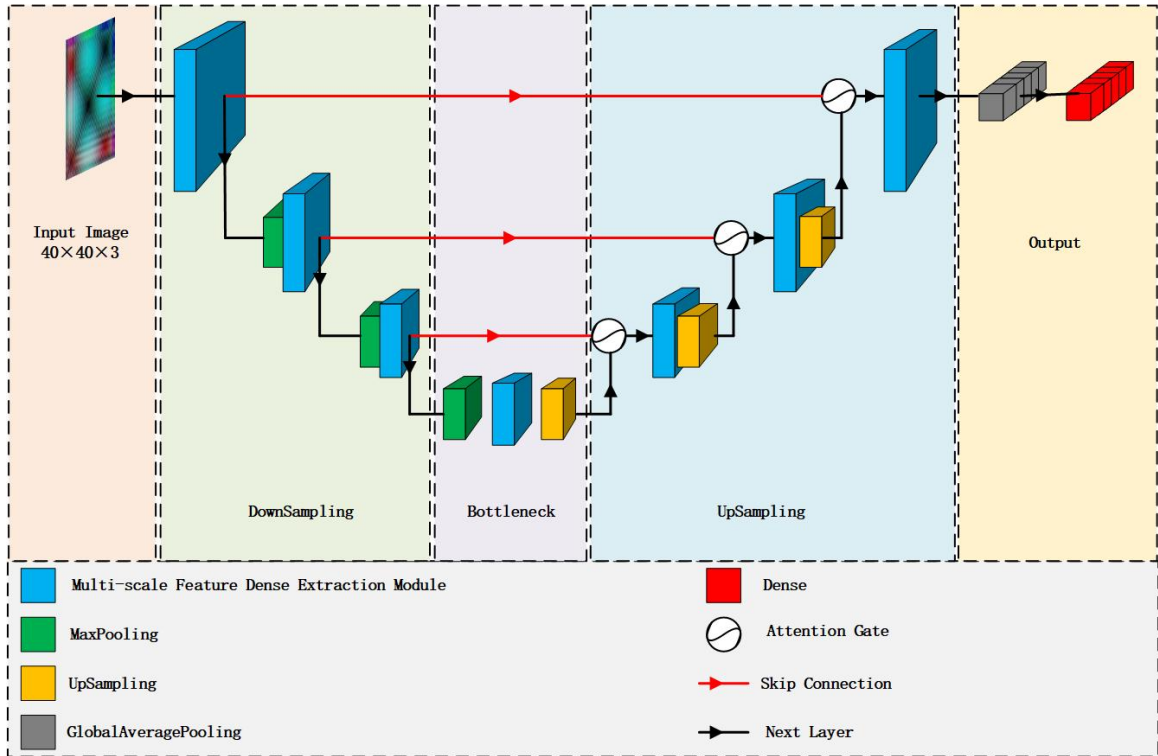


Fig. 5. Proposed deep-learning-based load recognition network.

### C. Proposed Deep Load Recognition Network

To recognize all loads from  $I_F$ , a critical issue is how to effectively extract both global and local features and avoid the influence of noises. To this end, we propose a deep load recognition network based on multi-scale features and attention mechanism. As shown in Fig. 5, the proposed network is a U-shape model with four stages: downsampling, bottleneck, upsampling and output.

In downsampling stage, the inputted  $I_F$  is sequentially processed by three attention-based Multi-scale Feature Dense Extraction Modules (MFDEMs) with max pooling operations by 2. We design the MFDEM with attention mechanism and multi-scale feature extraction, with its network structure shown in Fig. 6. First, it utilizes a  $1 \times 1$  convolution to extract coarse-grain features and further divides them into four feature subsets with the same space size. Second, it employs four different convolution kernels to extract features from different sub-sets:

$$b_i = \begin{cases} a_i & i = 1 \\ m_i(b_{i-1} + a_i) & 2 \leq i \leq 4 \end{cases} \quad (10)$$

where  $m_2()$ ,  $m_3()$  and  $m_4()$  are  $3 \times 3$ ,  $5 \times 5$  and  $7 \times 7$  convolutions, respectively. Third, it concatenates all inputs  $b_i, i \in [1, 4]$  and uses a  $1 \times 1$  convolution to fuse all features from different scales. Fourth, it employs attention mechanism to adaptively allocate weights to multi-scale features. By using three MFDEMs, the proposed network deeply exploits the image features at different scales that benefit the feature extraction ability of our model.

The attention network uses an average pooling to obtain a feature map with global reception field to represent the

importance of all channels. Then, it adds two fully connected layers and a ReLU function to introduce non-linearity in importance maps. Finally, it uses the Sigmoid function to generate new weights of channels and multiplies them with the original features to obtain the attention-based features. Obviously, the weighting operation of feature maps highlights important features and depresses the other features, thus it degrades the impacts of non-relevant features in load recognition.

In bottleneck stage, the downsampled features are processed by a max pooling, an MFDEM module and an Upsampling operation. Note that our network is a U-shape model that the output of each MFDEM is also fed to the upsampling stage with skip connection. This is to retain features of all scales, include both low-level and high-level features, which may benefit the load recognition to the extent possible. The bottleneck stage is set at the bottom of this U-shape model.

In upsampling stage, the features are processed as an inverse path of downsampling stage that consists of MFDEMs and upsampling operations by 2. As discussed in last paragraph, skip connections are introduced to feed features from downsampling stage. However, a direct addition of these features would be ineffective in recognition. Here we introduce an Attention Gate (AG) before each addition operation to selectively enhance low-level features. Fig. 7 shows the network structure of GA, where the low-level feature from skip connection (denoted by  $F_L$ ) is set as the gate control signal, and the high-level feature (denoted by  $F_H$ ) is used as the input signal. Both two signals are separately convoluted by  $1 \times 1$  and added into a new signal. Then, the new signal is activated by ReLU function, convoluted by  $1 \times 1$  and filtered by a Sigmoid function to obtain a weight matrix. Finally, the feature  $F_H$  is multiplied with the

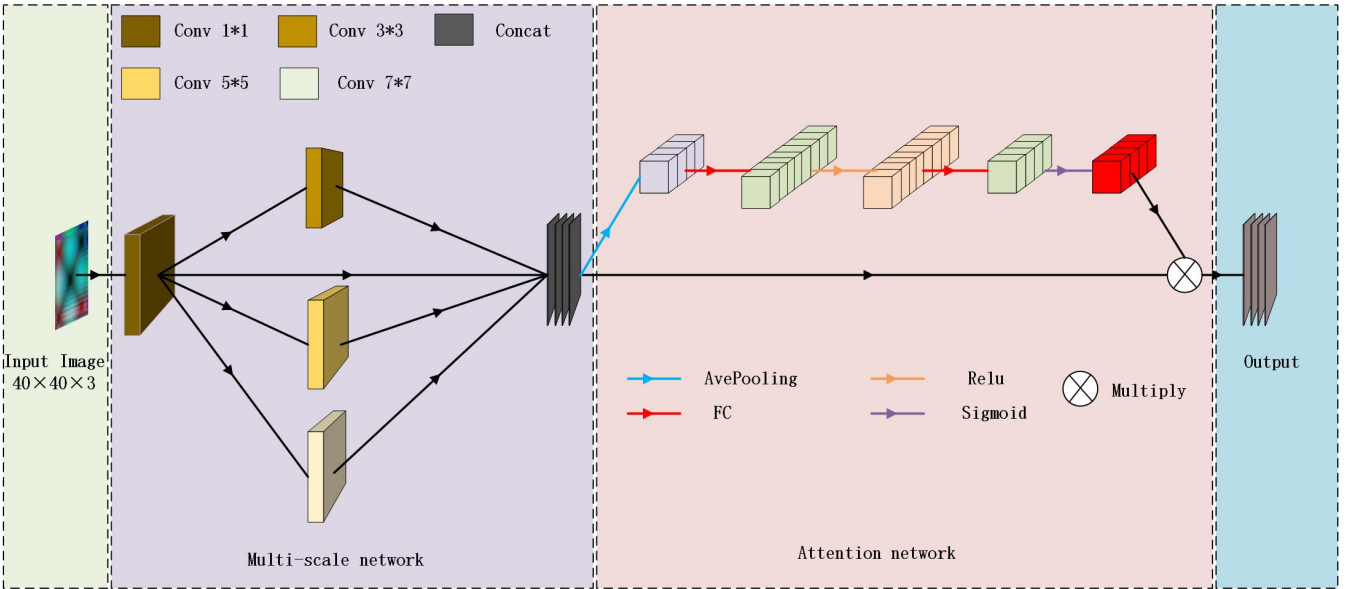


Fig. 6. Proposed Network of MFDEM.

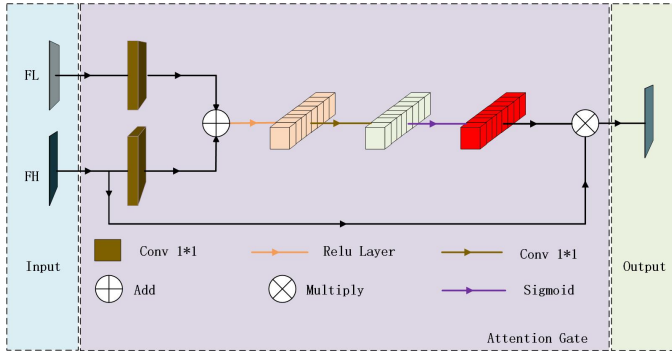


Fig. 7. Network of AG.

above weight matrix to obtain a new feature  $F_N$  that embodies both low-level and high-level features for load recognition.

The last stage outputs load recognition results based on the fused multi-scale features. It utilizes a global average pooling, a fully connected layer and a Softmax function to classify all types of loads. The average max pooling operation can further increase the perception field for recognition and also output a smaller parameter size for the following calculation. The fully connected layer with Softmax is commonly used in classification and recognition tasks due to its effectiveness in non-linear regression.

#### D. Smart Energy Management with Our Method

In summary, the steps of proposed load recognition method are as follows.

Step 1. Obtain the current signal  $c(n)$ .

Step 2. Calculate the three feature sequences, approximation coefficient  $S_a(n)$ , detail coefficient  $S_d(n)$  and harmonic content  $S_h(k)$ , with Eqs. (2), (3) and (5).

Step 3. Use the GAF method, as shown in Eqs. (6)-(9) to convert these feature sequences into a color image  $I_F$ .

Step 4. Identify the electric load with the image  $I_F$  and the proposed deep network in Fig. 5.

A practical AI-driven load management system can be implemented with our proposed load recognition method. As shown in Fig. 8, it is designed as a joint Terminal-Network-Could infrastructure for smart city. At the terminal-end, a load sensing and control terminal is in charge of managing all loads in a family or cell. On one hand, it collects load information (e.g. the current signal) and sends them to cloud server for further analysis; on the other hand, it receives and executes all commands from cloud server to control all loads for energy saving. The network is utilized to transmit all data and commands. Generally, it can be designed based on Narrow Band IoT (NB-IoT) for its low-power design, or 5G for its high transmission speed. At the cloud-end, a cloud-based service platform is responsible for load recognition, monitoring and control. It checks and analyzes the electricity consumption of all loads and provides suggestions on smart control of switches. Through its control, we are able to avoid unnecessary (e.g. lighting under daylight) or dangerous (e.g. abnormal use in factory) usage of electricity loads. Through this design, we expect to support efficient electricity management over large-scale IoT in smart city.

## IV. EXPERIMENTS AND SIMULATIONS

To examine the performance of our method, we compare it with the state-of-the-art methods on popular datasets. We also present the ablation studies to validate the effectiveness of our network design.

### A. Datasets

We compare all methods in a publicly available dataset, Plug Load Appliance Identification Dataset (PLAID) [30], with electric usage data of 11 types of loads. To increase the data samples for training, we also design a load sensing terminal

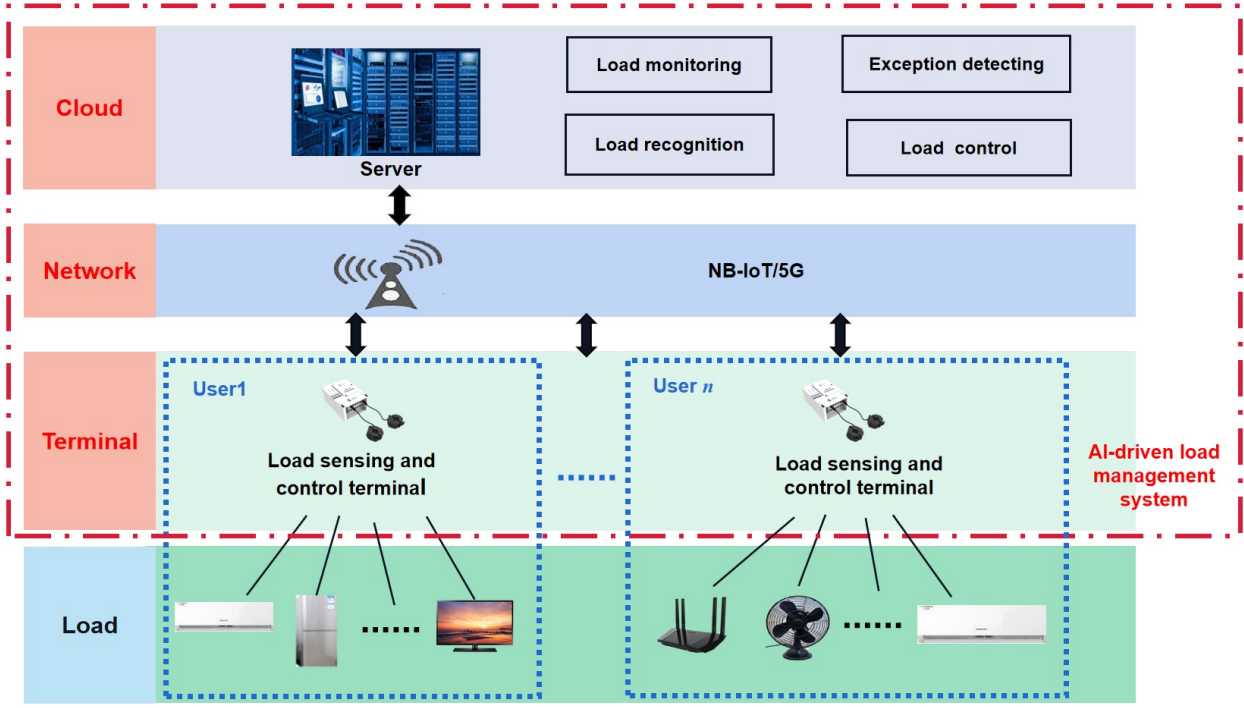


Fig. 8. Framework of the proposed AI-driven load management system.

and capture electric usage of 12 types of popular loads. The powers of these loads range from 24W to 1800W, which are representative to test the LRAs under similar electric loads or masking effect of loads.

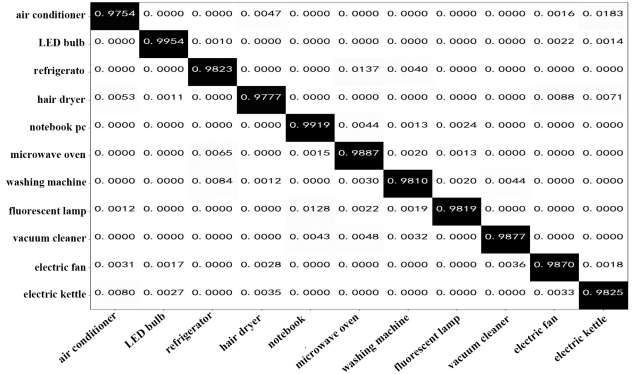
### B. The Performance of Our Method

The tested results of our method are summarized in Table I, including results on both PLAID and our datasets. For each dataset, we split it into a 70:30 ratio for training and testing. From the table, our method achieves a promisingly high accuracy of 98.26% on our dataset with an F1 score of 0.9819. It also achieves an accuracy of 97.71% and an F1 score of 0.9743 on the PLAID dataset. These results have fully demonstrated the efficiency of our load recognition model.

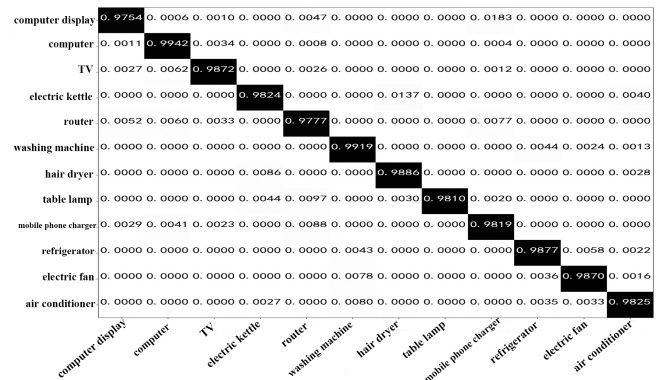
TABLE I  
PERFORMANCE OF OUR METHOD

Database	Accuracy	Precision	Recall	F1
Ours	0.9826	0.9818	0.9821	0.9819
PLAID	0.9771	0.9779	0.9707	0.9743

To analyze the recognition accuracies of different types of loads, we present the confusion matrixes on testing sets in Fig. 9. From the figure, all resistive loads, e.g. electric kettle (1800W) and hair dryer (1200W), can be well recognized with a high accuracy of 98.20%. This fact is mainly attributed to their distinct features of high powers and low harmonic contents. As discussed in Section III.B, pump-driven loads have similar feature distributions to those of motor-driven loads. In these categories, our model successively identifies



(a) Results on our dataset.



(b) Results on the PLAID dataset.

Fig. 9. Confusion matrixes of our method.

washing machine, electric fan, air conditioner and vacuum cleaner with a low probability of incorrect recognition or confusion. switching-powered loads have high harmonic contents, but also with low powers that might be covered by high-power loads. From the figure, our method is well capable of addressing this issue. Its recognition accuracies of notebook, TV and router exceed 96.88% even when high-power loads (*e.g.*, electric kettle, air conditioner) are working at full powers.

### C. Comparison with Popular Methods

To examine the superiority of our proposed method, we compare it with references [22-24] under the same conditions. The evaluation results on PLAID dataset are shown in Table II. From the table, our method surpasses all compared algorithms on PLAID with an average accuracy of 97.71%. This fact validates the effectiveness of our method in electric load recognition. It is thus capable of identifying all types of loads after a fine training in a large-scale electricity management system for smart city.

TABLE II  
COMPARISON RESULTS ON THE PLAID DATASET

Method	Network	Accuracy(%)
De's [22]	CNN	91.74
Liu's [23]	AlexNet	95.40
Ding's [24]	CNN	96.63
Ours	U-shape	97.71

In addition, both the two stages of our model, current feature visualization and deep load recognition, contribute to the final performance. With our current feature visualization and Ding's CNN model, the hybrid method also achieves an accuracy of 96.91% that outperforms Ding's method. By using both current feature visualization and deep load recognition, our method outperforms Ding's by 1.08%. This fact also validates our design.

### D. Ablation Study

We also perform ablation experiments to examine the design of our deep load recognition network. Experiments are run on both PLAID and our dataset.

*The effectiveness of multi-scale feature extraction:* Our deep network utilized multi-scale convolution kernels  $1\times 1$ ,  $3\times 3$ ,  $5\times 5$ ,  $7\times 7$ , as shown in Fig. 6. To validate its effectiveness, we compare it with identical kernel settings, *e.g.*  $1\times 1$ ,  $3\times 3$ ,  $5\times 5$  or  $7\times 7$ , with results summarized in Table III. All settings are retrained for fair comparison. From the table, our multi-scale feature extraction design is superior to all other settings. Therefore, our deep model can well extract all critical information from the visualized current and thus is more suitable for load recognition.

*The effectiveness of Attention Gate:* The AGs are utilized to add multi-scale features after skip connections. From Table IV, our method achieves inferior performance without these AGs. Therefore, both multi-scale feature extraction and attention mechanism contribute to the final recognition performance.

TABLE III  
PERFORMANCE EVALUATION WITH DIFFERENT KERNELS

Kernel	Accuracy	Precision	Recall	F1
$1\times 1$	0.85100	0.85611	0.85076	0.85342
$3\times 3$	0.92458	0.92573	0.92184	0.92378
$5\times 5$	0.95333	0.95576	0.94941	0.95257
$7\times 7$	0.95497	0.95720	0.95393	0.95566
Ours	0.98465	0.98681	0.98114	0.98396

TABLE IV  
PERFORMANCE EVALUATION W/ AND W/O AGS

	Parameters	Accuracy	Precision	Recall	F1
w/ AG	1264014	0.98465	0.98681	0.98114	0.98396
w/o AG	1247515	0.97497	0.97481	0.97235	0.97357

### E. Discussion on Practical Use

As shown in Fig. 8, our method can be deployed at the cloud-end of smart city. The system embodies a joint Terminal-Network-Cloud infrastructure where a load monitoring and management system that surveils power on/off and electric usage of loads for each family/cell, and also controls the electric usage if necessary. At the terminal-end, the system captures all required information of electric usage; while at the cloud-end, the system identifies all working loads, analyzes the regional or local electric consumption and sends controlling commands if necessary. Note the cloud-server runs our NILM method only if necessary. Thus, the computational cost is not a critical issue. Actually, our experiments also show that we are able to run this NILM approach on a laptop, which is reasonable because our deep model processes a  $40\times 40$  color image only. As a result, the proposed NILM approach can be deployed in the smart electricity management system of smart city.

## V. CONCLUSION

This paper proposes a NILM method based on current feature visualization and deep recognition network. It first converts current signals into color images with a combination of signal transform and GAF method. Then, it utilizes multi-scale feature extraction and attention mechanism to design a U-shape recognition network. Experimental results demonstrate its efficiency in both public and our own datasets, as well as its performance superiority compared with its peers. The proposed method can be embedded into the load monitoring and management system to control the electric usage and save energy in smart city.

## REFERENCES

- [1] C. S. Lai, T. I. Strasser, and L. L. Lai, "Editorial to the special issue on smart cities based on the efforts of the systems, man, and cybernetics society," *IEEE Transactions on Systems, Man, and Cybernetics: Systems*, vol. 52, no. 1, pp. 2-6, 2022.



- [2] V. C. Paes, C. H. M. Pessoa, V. C. Farias Da Costa, L. F. S. Oliveira, and J. M. De Souza, "IoE knowledge flow model in smart cities," in *2022 IEEE International Conference on Systems, Man, and Cybernetics (SMC)*, 2022, pp. 982–987.
- [3] X. He, D. W. C. Ho, T. Huang, J. Yu, H. Abu-Rub, and C. Li, "Second-order continuous-time algorithms for economic power dispatch in smart grids," *IEEE Transactions on Systems, Man, and Cybernetics: Systems*, vol. 48, no. 9, pp. 1482–1492, 2018.
- [4] I. Zenginlis, J. Vardakas, N. E. Koltsaklis, and C. Verikoukis, "Smart home's energy management through a clustering-based reinforcement learning approach," *IEEE Internet of Things Journal*, vol. 9, no. 17, pp. 16 363–16 371, 2022.
- [5] W. Han, X. S. Lu, M. Zhou, X. Shen, J. Wang, and J. Xu, "An evaluation and optimization methodology for efficient power plant programs," *IEEE Transactions on Systems, Man, and Cybernetics: Systems*, vol. 50, no. 2, pp. 707–716, 2020.
- [6] A. E. Lazzaretti, D. P. B. Renaux, C. R. E. Lima, B. M. Mulinari, H. C. Ancelmo, E. Oroski, F. Pöttker, R. R. Linhares, L. d. S. Nolasco, L. T. Lima *et al.*, "A multi-agent nilm architecture for event detection and load classification," *Energies*, vol. 13, no. 17, p. 4396, 2020.
- [7] J. He, Z. Zhang, L. Zhu, Z. Zhu, J. Liu, and K. Gai, "An efficient and accurate nonintrusive load monitoring scheme for power consumption," *IEEE Internet of Things Journal*, vol. 6, no. 5, pp. 9054–9063, 2019.
- [8] M. Ghaffar, S. R. Sheikh, N. Naseer, Z. M. U. Din, H. Z. U. Rehman, and M. Naved, "Non-intrusive load monitoring of buildings using spectral clustering," *Sensors*, vol. 22, no. 11, p. 4036, 2022.
- [9] Z. Lu and S. Shaowei, "A non-intrusive load monitoring method based on multi-scale wavelet packet optimization and transient feature matching," in *2021 12th IEEE International Conference on Software Engineering and Service Science (ICSESS)*. IEEE, 2021, pp. 113–117.
- [10] L. Yan, J. Han, H. Wang, Z. Li, and Z. Li, "An online transient-based electrical appliance state tracking method via markov chain monte carlo sampling," in *2020 IEEE Power and Energy Society General Meeting (PESGM)*. IEEE, 2020, pp. 1–5.
- [11] K. Basu, V. Debusschere, A. Douzal-Chouakria, and S. Bacha, "Time series distance-based methods for non-intrusive load monitoring in residential buildings," *Energy and Buildings*, vol. 96, pp. 109–117, 2015.
- [12] P. G. Papageorgiou, P. A. Gkaidatzis, G. C. Christoforidis, and A. S. Bouhouras, "Unsupervised nilm implementation using odd harmonic currents," in *2021 56th International Universities Power Engineering Conference (UPEC)*. IEEE, pp. 1–6.
- [13] T. Ji, L. Liu, T. Wang, W. Lin, M. Li, and Q. Wu, "Non-intrusive load monitoring using additive factorial approximate maximum a posteriori based on iterative fuzzy *c*-means," *IEEE Transactions on Smart Grid*, vol. 10, no. 6, pp. 6667–6677, 2019.
- [14] B. Liu, W. Luan, and Y. Yu, "Dynamic time warping based non-intrusive load transient identification," *Applied energy*, vol. 195, pp. 634–645, 2017.
- [15] H. Kang, H. Kim *et al.*, "Household appliance classification using lower odd-numbered harmonics and the bagging decision tree," *IEEE Access*, vol. 8, pp. 55 937–55 952, 2020.
- [16] S.-H. Yi, J. Wang, and J.-J. Liu, "Simultaneous load identification method based on hybrid features and genetic algorithm for nonintrusive load monitoring," *Mathematical Problems in Engineering*, vol. 2022, pp. 1–13, 2022.
- [17] T.-T.-H. Le, S. Heo, and H. Kim, "Toward load identification based on the hilbert transform and sequence to sequence long short-term memory," *IEEE Transactions on Smart Grid*, vol. 12, no. 4, pp. 3252–3264, 2021.
- [18] D. Saha, A. Bhattacharjee, D. Chowdhury, E. Hossain, and M. M. Islam, "Comprehensive nilm framework: device type classification and device activity status monitoring using capsule network," *IEEE Access*, vol. 8, pp. 179 995–180 009, 2020.
- [19] K. Li, B. Yin, Z. Du, and Y. Sun, "A nonintrusive load identification model based on time-frequency features fusion," *IEEE Access*, vol. 9, pp. 1376–1387, 2020.
- [20] B. Yin, L. Zhao, X. Huang, Y. Zhang, and Z. Du, "Research on non-intrusive unknown load identification technology based on deep learning," *International Journal of Electrical Power & Energy Systems*, vol. 131, p. 107016, 2021.
- [21] D. Jia, Y. Li, Z. Du, J. Xu, and B. Yin, "Non-intrusive load identification using reconstructed voltage-current images," *IEEE Access*, vol. 9, pp. 77 349–77 358, 2021.
- [22] L. De Baets, J. Ruysinck, C. Develder, T. Dhaene, and D. Deschrijver, "Appliance classification using vi trajectories and convolutional neural networks," *Energy and Buildings*, vol. 158, pp. 32–36, 2018.
- [23] Y. Liu, X. Wang, and W. You, "Non-intrusive load monitoring by voltage-current trajectory enabled transfer learning," *IEEE Transactions on Smart Grid*, vol. 10, no. 5, pp. 5609–5619, 2018.
- [24] H. Ding, Y. Le, S. Hongling, and S. Hong, "Realize intelligent non-intrusive load identification by using data visualization," *Journal of Huazhong University of Science and Technology (Nature Science Edition)*, pp. 010–049, 2021.
- [25] M. Wenninger, S. P. Bayerl, A. Maier, and J. Schmidt, "Recurrence plot spacial pyramid pooling network for appliance identification in non-intrusive load monitoring," in *2021 20th IEEE International Conference on Machine Learning and Applications (ICMLA)*. IEEE, 2021, pp. 108–115.
- [26] S. Temel, N. Unaldi, and O. Kaynak, "On deployment of wireless sensors on 3-d terrains to maximize sensing coverage by utilizing cat swarm optimization with wavelet transform," *IEEE Transactions on Systems, Man, and Cybernetics: Systems*, vol. 44, no. 1, pp. 111–120, 2014.
- [27] X.-y. Zhang and R.-j. Zhang, "The technology research in decomposition and reconstruction of image based on two-dimensional wavelet transform," in *2012 9th International Conference on Fuzzy Systems and Knowledge Discovery*. IEEE, 2012, pp. 1998–2000.
- [28] H. H. S. M. Ali and S. M. Sharif, "Computation reduction of haar wavelet coefficients," in *2017 2nd International Conference on Image, Vision and Computing (ICIVC)*, 2017, pp. 832–835.
- [29] S. Moshe and D. Hertz, "On computing dft of real n-point vector and idft of dft-transformed real n-point vector via single dft," *IEEE Signal Processing Letters*, vol. 6, no. 6, pp. 141–, 1999.
- [30] J. Gao, S. Giri, E. C. Kara, and M. Bergés, "Plaid: a public dataset of high-resolution electrical appliance measurements for load identification research: demo abstract," in *proceedings of the 1st ACM Conference on Embedded Systems for Energy-Efficient Buildings*, 2014, pp. 198–199.